



Occurrence of upslope flows at the Pico mountaintop observatory: A case study of orographic flows on a small, volcanic island

J. Kleissl,^{1,2} R. E. Honrath,³ M. P. Dziobak,³ D. Tanner,⁴ M. Val Martín,³
R. C. Owen,³ and D. Helmig⁴

Received 30 May 2006; revised 8 October 2006; accepted 9 November 2006; published 22 February 2007.

[1] Upslope flows caused by mechanical forcing in strong synoptic winds or by buoyant forcing driven by solar heating under weak synoptic winds can influence the air composition at mountaintop observatories. Using meteorological and trace gas measurements at the PICO-NARE observatory on Pico mountain (Azores Islands, North Atlantic Ocean), the frequency and impact of such orographic flows on a small, volcanic, subtropical island was examined. To determine the origin of mechanically lifted air, upstream kinetic energy was balanced against potential energy gained during uplift (Sheppard's model). Mechanically forced upslope flow is most important during October through April, when the calculated probability of observing marine boundary layer (MBL) air at the observatory near the summit ranges from 35 to 60% per month. In contrast, lower synoptic wind speeds and a more stable lower free troposphere during May–September result in a reduced frequency of MBL impacts (<20%). Buoyant upslope flows (BUF) were quantified through meteorological measurements on the mountain slope in summer 2004. Diurnal cycles of wind direction on the mountain slope consistent with daytime upslope and nighttime downslope flow were found on 24% of the days during late June, July, and August 2004. Buoyant forcing can also occur in the presence of moderate synoptic winds, resulting in enhancement of the mechanically forced upslope flow on the windward side of the mountain. Such conditions were found on 15% of the summer days in 2004. However, on BUF days the specific humidity at the mountaintop was significantly smaller than on the slope, indicating turbulent mixing during ascent or vertical decoupling of air masses. Impacts of BUF or a mixture of buoyant and mechanical upslope flow on O₃ or nitrogen oxides mixing ratios at the mountaintop station were rare or extremely small, and no significant diurnal cycle of O₃ (expected if daytime BUF of MBL air occurred regularly) was present. Midday increases in isoprene concentrations, a nonmethane hydrocarbon (NMHC) expected to be emitted from vegetation more than 700 m below the PICO-NARE station, were found on 54% of the days during May–August 2005. No corresponding increase in *n*-butane (used for heating and cooking at sea level residences) was detected, suggesting that the air did not originate from as low as sea level. These results indicate that the latitude, size, and topography of Pico island combine to prevent frequent transport of MBL air to the PICO-NARE station in the summer.

Citation: Kleissl, J., R. E. Honrath, M. P. Dziobak, D. Tanner, M. Val Martín, R. C. Owen, and D. Helmig (2007), Occurrence of upslope flows at the Pico mountaintop observatory: A case study of orographic flows on a small, volcanic island, *J. Geophys. Res.*, *112*, D10S35, doi:10.1029/2006JD007565.

¹Department of Mechanical and Aerospace Engineering, University of California, San Diego, La Jolla, California, USA.

²Formerly at Department of Civil and Environmental Engineering, Michigan Technological University, Houghton, Michigan, USA.

³Department of Civil and Environmental Engineering, Michigan Technological University, Houghton, Michigan, USA.

⁴Institute of Arctic and Alpine Research, University of Colorado, Boulder, Colorado, USA.

1. Introduction

[2] Many atmospheric observatories are located on mountains, with the aim of observing conditions in the free troposphere (FT). Such observations are valuable for the determination of background mixing ratios and trends of tropospheric trace gases and for studies of long-range impacts of upwind source regions [e.g., Oltmans *et al.*, 1998; Scheel *et al.*, 1998; Zanis *et al.*, 1999; Fischer *et al.*, 2004; Ridley and Robinson, 1992; Igarashi *et al.*, 2004;

Schmitt and Volz-Thomas, 1997]. However, correct interpretation of mountaintop or mountainside measurements requires an understanding of upslope flow, which is of concern for several reasons [e.g., *Ryan*, 1997; *Fischer et al.*, 1998; *Tsutsumi et al.*, 1994]. First, it can bring pollutant emissions from low-altitude towns and roadways to high altitudes, contaminating the desired background measurements. Alternatively, in the absence of nearby emission sources it can lift clean boundary layer air, which typically has a composition different than that in the FT [e.g., *Hahn et al.*, 1992; *Oltmans et al.*, 1996; *Peterson et al.*, 1998]. Finally, more moderate upslope lifting may result in the sampling of FT air characteristic of an altitude lower than station altitude, which may have different composition as a result of air mass layering in the FT [e.g., *Oltmans et al.*, 1996; *Ridley et al.*, 1997]. In this work, our focus is on the effects of upslope flow on the most simple type of mountain stations: those on islands. Our particular focus is the occurrence of upslope flows that may impact observations at the PICO-NARE station located on Pico mountain in the central North Atlantic Azores Islands. Upslope flow on isolated mountains results from two primary mechanisms, mechanically forced lifting and buoyant upslope flow, which provide the energy needed to overcome the stable stratification typically present in the FT.

1.1. Mechanically Forced Lifting

[3] Mechanically forced lifting results from the deflection of strong winds by the mountain slope, with the energy driving the upslope flow originating in the upwind wind field. Most of the research on mechanically forced lifting has focused on laboratory experiments or numerical simulations [e.g., *Snyder*, 1985; *Ding et al.*, 2003]. Only a small number of field studies have been conducted, mostly on small hills where the original height of a fluid parcel is hard to quantify because of small differences in potential temperature and specific humidity over the height of the mountain [*Jenkins et al.*, 1981; *Spangler*, 1987; *Taylor and Teunissen*, 1987].

[4] The nondimensional mountain height, $h_{ND} = hN/U_\infty = Fr^{-1}$ is the most important parameter to classify mechanically forced stratified flows over mountains [e.g., *Ding et al.*, 2003; *Hunt and Snyder*, 1980]. Here, $N^2 = g/T_v \times \partial\theta/\partial z$ is the Brunt-Vaisala frequency squared, $T_v(z)$ is the virtual temperature, $\theta(z)$ is the potential temperature, U_∞ is the horizontal velocity upstream of the mountain, h is the mountain height, g is the gravitational constant, and z is altitude. If $h_{ND} \gtrsim 1$, upstream blocking will occur, with the large-scale flow dividing into two parts, the lower part traveling around the mountain and the upper part flowing over the mountain. The streamline separating these two parts is termed the dividing streamline, and its height upstream of the mountain is termed z_t .

[5] Thus an air parcel above the dividing streamline will flow over the mountain, while air parcels below the dividing streamline, though they will be lifted to some degree, will ultimately flow around the mountain. This behavior has important implications for air sampling on mountains, as a plume present below z_t will not reach the mountaintop, but will disperse horizontally, while a plume present above z_t will be lifted over the mountain, and will disperse vertically

in the wake of the mountain or through gravity wave breaking.

[6] The importance of mechanically driven upslope flow varies among mountains, depending mainly on mountain height and the mean wind speed. Thus some smaller mountains subject to strong winds and/or weak stratification may experience $h_{ND} \ll 1$, resulting in uplift of nearly all upwind air over the mountain. In contrast, some large mountains (including Mauna Loa, discussed below) in weak winds and/or strong stratification experience $h_{ND} \gg 1$, with the result that mechanically driven uplift is less important, because z_t is close to the mountain height.

[7] However, mountains with moderate nondimensional heights experience mechanically driven upslope flow of varying degrees. For measurement stations on such mountains, estimation of the dividing streamline height is necessary to characterize the origin altitude of the air sampled.

[8] z_t can be estimated from data available from soundings or numerical weather models by using *Sheppard's* [1956] model, which is based on Bernoulli's law. *Sheppard* [1956] postulated that the reduction in kinetic energy along a streamline flowing over a mountain is balanced by the resulting increase in potential energy. This results in the following equation

$$\frac{1}{2}U_\infty^2(z_t) = \int_{z_t}^h (h-z)N^2(z)dz, \quad (1)$$

which may be iteratively solved for z_t . (In the case of constant $U_\infty(z)$ and constant $N(z)$, equation (1) simplifies to $z_t = h [1 - U_\infty/Nh]$. Thus $z_t/h = 1 - U_\infty/Nh = 1 - Fr$, and the air that reaches the mountaintop has been lifted by $h - z_t = U_\infty/N$.)

[9] When condensation occurs during lifting, i.e., when the lifting condensation level (LCL) of air originating at z_t is below h , latent heating must be taken into account in the determination of z_t . This can be accomplished through the use of a wet buoyancy frequency [*Durran and Klemp*, 1982].

$$\frac{1}{2}U_\infty^2(z_t) = \int_{z_t}^{LCL(z_t)} (h-z)N^2(z)dz + \int_{LCL(z_t)}^h (h-z)N_w^2(z)dz, \quad (2)$$

where

$$N_w^2 = \frac{g}{T} \left(\frac{dT}{dz} + \Lambda_m \right) \left(1 + \frac{L_v q}{RT} \right) - \frac{g}{1 + q_w} \frac{dq_w}{dz}. \quad (3)$$

T is the sensible temperature, Λ_m is the moist adiabatic lapse rate, L_v is the latent heat of vaporization, q_w is the total specific humidity, and R is the ideal gas constant for dry air. *Jiang* [2003] recommended that the moist N_m from the background flow be estimated from equation (2) by assuming that the flow is saturated, but no liquid water exists ($q_w = q_{sat}$).

[10] Implicit in *Sheppard's* approximation are several assumptions that are known to be violated to some degree: that the flow is inviscid, that pressure perturbations at the summit of the hill are negligible, and that effects of the

shape of the mountain are unimportant [Smith, 1988]. Nevertheless, the model has been shown to provide a reasonable description of the degree of uplift. On the basis of numerical simulations of inviscid flow, Ding *et al.* [2003] concluded that the model is successful because “the energy provided by pressure field roughly offsets the energy loss due to friction/turbulence for axisymmetric hills.” We recently analyzed the accuracy of z_t estimates from Sheppard’s formula, using observations of clouds, specific humidity, and temperature at the PICO-NARE station that is the subject of this paper [Kleissl *et al.*, 2006]. The results confirmed the findings of other investigators [Hunt and Snyder, 1980; Vosper *et al.*, 1999; Ding *et al.*, 2003] that z_t predictions from Sheppard’s model are generally accurate, with a tendency to slightly overestimate the degree of uplift.

1.2. Buoyant Upslope Flow

[11] The second type of upslope flow, buoyant upslope flow (BUF), results from daytime solar heating of air near the surface of the mountain causing it to rise toward the summit. At night, radiative cooling of the surface leads to gravity flows down the mountain. This diurnal pattern typically occurs in conditions of weak synoptic winds and clear skies. Buoyantly driven flows of both the upslope (anabatic) and downslope (katabatic) types are important to mountain meteorology and air pollutant transport [e.g., Whiteman, 2000; Furger *et al.*, 2000]. While our focus here is on upslope flows, downslope flows may be of importance to observatories on the sides, rather than the summit, of mountains. BUFs near isolated mountains are relatively simple, though flows in mountain-valley regions can be quite complex [Whiteman, 1990; Chen and Nash, 1994]. Typically, BUF occurs on all (nonshaded) sides of the mountain, producing a “chimney” effect, and it is expected to be strongest on the side with the highest net radiation (the difference between incoming and outgoing radiation).

[12] BUFs are often stronger near mountains on islands than over continents, because of the supportive effect of differential heating between island and ocean [Whiteman, 2000]. During the day, land heats to a much greater extent than does the ocean, causing an onshore sea breeze. This near-surface flow supports the mountain-induced BUF, with a compensating return flow at higher elevations.

1.3. Upslope Flow at Selected Mountain Observatories

[13] The forcing mechanisms responsible for mechanically driven and buoyant upslope flows are complementary, with mechanically driven upslope flow most important during periods of high synoptic wind speeds and low insolation, and BUF strongest during the afternoons of cloud-free summer days with weak or calm synoptic winds. However, on any given mountain the importance of each mechanism also depends on seasonally varying climate and on mountain size and shape.

[14] Mauna Loa Observatory (MLO), a mountain station where upslope flows have been well studied, provides a useful point of comparison for the present study. MLO is located on the island of Hawaii, at 3.4 km on the north slope of the 4.2 km Mauna Loa volcano. This elevation is above that of the trade wind inversion typically present in this region (~ 2 – 2.6 km). Mechanically forced lifting is of minimal importance there, as the nondimensional mountain height

h_{ND} is typically in the range of 4 to 8, on the basis of typical trade wind conditions ($U_\infty = 5$ to 10 m s^{-1} and $N \sim 0.013 \text{ s}^{-1}$) and aerodynamic mountain height $h \sim 3130 \text{ m}$ [Rasmussen *et al.*, 1989]. Thus Chen and Nash [1994] determined that the northwesterly tradewinds decelerate on the windward slopes and the flow splits around Hawaii island.

[15] Buoyancy-driven flows are of prime importance on Hawaii, however, and dominate the flow regime, as a result of the large island size (diameter $\sim 140 \text{ km}$), high insolation rates at the island’s low latitude (19°N), and the barren, low albedo slopes of Mauna Loa and adjacent Mauna Kea volcanoes [Carbone *et al.*, 1995; Ryan, 1997]. Mendonca [1969] analyzed 8 years of meteorological measurements at MLO and demonstrated the persistence of the diurnal cycle resulting from buoyant upslope and downslope flows. Nighttime downslope flows occurred on 90% of all days, independent of season, while solar heating-driven upslope flows were more frequent and faster in July (78%) than in January (52%). At the station, the onset of upslope flow each morning was preceded by a brief period of calm winds and was followed first by dry, FT air (transported down the mountain by downslope flow the previous night) and second by more humid air carried up from lower elevations. The upslope flow intensified in the early afternoon and brought increasingly moist air to the observatory, leading on days with weak trade-wind inversions to scattered orographic clouds. Finally, the process reversed at sunset, with a brief period of calm winds followed by downslope flow.

[16] A number of investigators have attempted to quantify the elevation of origin of upslope flow to MLO and the resulting impact on chemical measurements there. Hahn *et al.* [1992] compared dew point temperatures at Mauna Loa with those from soundings nearby. Nearly all days in May 1988 exhibited a similar behavior, with nighttime dew points similar to those at 700 hPa (near the actual station elevation), but daytime dew points enhanced, on average consistent with the soundings near 780 hPa ($\sim 2200 \text{ m}$), well below the station. Ryan [1997] compared station measurements of both O_3 and dew point temperature to those from soundings. On average the station O_3 measurements were consistent with sounding observations at 3360 m (near station elevation) at night (0100 HST), but were displaced to 2650 m in the afternoon (at 1300 HST). However, there was a large degree of variability in the afternoon value, which correlated with variations in the height of the trade wind inversion. As a result, the apparent origin elevation was below the inversion top 72% of the time and within the marine boundary layer (MBL, i.e., below the inversion base) 15% of the time.

[17] These analyses suggest a potentially significant impact of upslope flow on chemical composition at MLO. Significant diurnal cycles that result from the upslope/downslope flow regime are indeed observed at the station. While O_3 is at a minimum in the afternoon as noted above, condensation nuclei, light alkenes, isoprene, and peroxyacetyl nitrate (PAN) are enhanced during upslope flow periods [e.g., Mendonca and Pueschel, 1973; Hahn *et al.*, 1992; Greenberg *et al.*, 1996]. The largely increased concentrations of ethene and propene in upslope flow indicated that upslope air had a strong contribution of marine boundary layer origin, as both of these compounds are deemed to result from marine sources [Greenberg *et al.*, 1996]. Con-

sistent with the dew point analyses, the afternoon extremes in these cycles lag 1.5–2 hours behind the upslope flow peak, indicating transport of subinversion, island-modified air. The daily cycles in these species are quite distinct. For example, O_3 (discussed below in the context of the PICO-NARE station) varied from a nighttime maximum of 44 ppbv to an afternoon minimum of 33 ppbv during May 1988 [Hahn *et al.*, 1992].

[18] These studies demonstrate that air from below the trade wind inversion impacts MLO during the daytime. However, the BUF is more complex than a simple conveyor belt traveling up the mountainside. Chen and Nash [1994] concluded that daytime heating rates were too small to account for air following the terrain up the mountainside, as rising air would be cooler than air further upslope, even allowing for the heat released from condensation. They suggested that low-elevation air could nevertheless impact the station as a result of lifting in thermals. As one example of the apparently complex nature of the upslope flow, Hübler *et al.* [1992] found daytime/nighttime differences in total reactive nitrogen oxides (NO_y) at MLO were smaller than expected if upslope flow simply carried MBL air to the station. They concluded that daytime air at MLO may instead be a mixture of island-modified MBL air and FT air.

[19] For practical purposes, however, it is not necessary to know the precise origin of air during upslope flow periods, since measurements in either island-modified MBL air or a poorly constrained mixture of MBL and FT air are not easily interpretable. For this reason, interpretations of chemical measurements at MLO usually exclude observations during upslope flow periods. Since the timing of upslope flow is so consistent at MLO, this can be done by applying a time of day filter, as described by Walega *et al.* [1992] who applied a filter consisting of a time constraint (2200–1000 HST) and the requirement that winds not be calm (wind speed at least 1 m s^{-1}).

[20] Finally in this introduction, we mention briefly two measurement locations closer to the PICO-NARE station. The Izaña Global Atmosphere Watch station is located on Tenerife island in the Canary Islands of the eastern North Atlantic. This station is somewhat farther north than MLO, but is also affected by the strong trade wind inversion. It is located at 2.4 km elevation on the 3.7 km Teide volcano. Upslope flow bringing air contaminated with island emissions significantly impacts measurements at Izaña, and only nighttime measurements there are clearly interpretable as a result [e.g., Fischer *et al.*, 1998; Rodriguez *et al.*, 2004]. For example, during the OCTA intensive (11–21 August 1993), average O_3 levels dropped from 55 ppbv at night (0000–0600 local time) to 50 ppbv in the afternoon (1200–1800 local time) [Fischer *et al.* 1998, Figure 5]. Afternoon changes were larger for species emitted by island sources. For example, CO increased from 88 to 113 ppbv and NO_y rose from approximately 400 pptv to more than 1 ppbv over the same period [Fischer *et al.*, 1998].

[21] Measurements made at the summit of the much smaller Sta. Barbara volcano on Terceira Island in the Azores Islands provide a sharp contrast to MLO and Izaña. The elevation of the peak of Sta. Barbara, 1.0 km, is usually within the MBL in this region (see below). The low elevation, in combination with the occurrence of mechanically forced upslope flow (annual median $h_{ND} \simeq 0.9$),

means that MBL air is expected to dominate at this location. Consistent with these expectations, no evidence that FT air was sampled was found during measurements in August 1993 (with the exception of a frontal event) [Peterson *et al.*, 1998]. However, daytime solar heating resulted in the uplift of island emissions to the mountaintop, significantly contaminating daytime measurements of NO_y . The magnitude of island impacts relative to MBL levels was much smaller for CO and O_3 , with the result that the amplitudes of the diurnal cycles of those species were very small (≤ 2 ppbv) [Parrish *et al.*, 1998].

[22] Common to these stations is the conclusion that the occurrence of upslope flow of boundary layer air and of local emissions must be carefully assessed in order to properly interpret trace gas measurements at mountain stations. In the remainder of this paper, we present the results of a study of the occurrence of upslope flow on Pico mountain in the Azores Islands and the resulting impact on measurements made at the PICO-NARE station. Conditions here differ from those at MLO and Izaña in several key respects. Most importantly, the station is significantly farther north (latitude 38.5°N) causing reduced insolation and buoyant forcing. Moreover, the island is smaller and not heavily populated, and the mountain is smaller. These differences result in increased importance of mechanically driven uplift and reduced importance of buoyant uplift. This study therefore provides an indication of the degree of variation in upslope flow impacts at mountain locations usable for atmospheric measurements, and provides a site characterization required for proper interpretation of measurements at the PICO-NARE station. Station measurements of O_3 , nitrogen oxides, CO, and nonmethane hydrocarbons (NMHC) are used in this work to assess the occurrence of mixing ratio changes resulting from upslope flow.

2. Methods

2.1. PICO-NARE Station Measurements

[23] The PICO-NARE station is located on Pico mountain, on Pico Island in the Portuguese Azores Islands (Figure 1). Pico mountain is of volcanic origin and has a nearly ideal conical shape, with an average slope of approximately 40° above 1250 m msl. The station is located at 2225 m approximately 50 m from the north end of a nearly flat, circular caldera with a diameter of approximately 500 m. The south and west sides of the caldera are bounded by a ~ 20 m rock wall, and a small volcanic cone centered approximately 300 m east-southeast extends an additional ~ 130 m vertically. Meteorological measurements at the PICO-NARE station are made routinely and are listed in Table 1. Wind measurements there are complicated by eddies resulting from wind flow over the cliff 50 m north of the station or over the caldera wall to the west and are not used here.

[24] O_3 was determined using a commercial ultraviolet absorption instrument (Thermo Environmental Instruments, Inc., Franklin Massachusetts, Model 49C), and CO was determined using a commercial instrument modified by the addition of a zeroing system (Thermo Environmental, Inc., Model 48C-TL). The absence of O_3 loss in the inlet line was verified once per day; CO instrument sensitivity was determined at the same time. Nitrogen oxides measurements

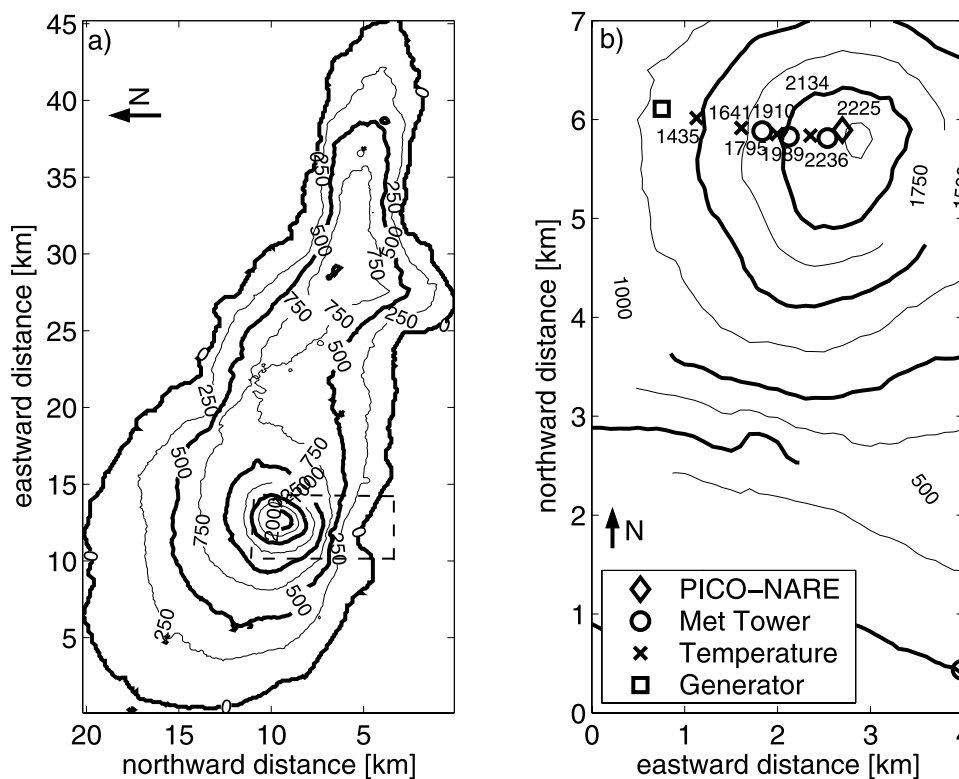


Figure 1. Topographical map of Pico from Shuttle Radar Topography Mission (SRTM) data (NASA, USGS, <http://seamless.usgs.gov>). Contours are spaced 250 m apart, from 0 to 2250 m. (a) Entire island. The PICO-NARE station is located at 38.47°N, 28.40°W at 2225 m, just northwest of the summit. Most of the terrain above 1250 m is bare lava soils, while most lower-lying areas are grasslands and mixed shrub and forested land cover types. The dashed lines show the boundaries of the map displayed in Figure 1b. (b) Pico mountain with the locations and elevations of the meteorological stations listed in Table 1. Crosses represent simple temperature stations, while circles indicate stations with several instruments. The square at 1253 m marks the location of the diesel generator, which powers the PICO-NARE station.

include NO, determined using a Michigan Tech ozone chemiluminescence instrument, NO₂, determined using the same instrument after photolysis to NO using a 300 W xenon lamp, and NO_y, determined as NO after Au-catalyzed reduction to NO in the presence of 0.3% (vol/vol) CO. NO_y and NO₂ conversion efficiencies and instrument sensitivities were determined twice daily. NMHC were routinely monitored using a cryogen-free gas chromatography system with a single-stage peltier-cooled adsorbent trapping unit. Samples were taken about every four hours throughout the day

[Tanner *et al.*, 2006]. More details on the chemical measurements are provided elsewhere in this special issue [Owen *et al.*, 2006; Val Martín *et al.*, 2006; D. Helmig *et al.*, unpublished manuscript, 2006].

2.2. Intensive Meteorological Measurements and Supporting Data

[25] Additional meteorological measurements to support this study were conducted during the period 27 June to 27 August 2004. Eight measurement stations were added, at the

Table 1. Meteorological Measurements on Pico Mountain From 27 June to 27 August 2004^a

Elevation, m MSL	Measured Variables	Instrumentation	Avg, min
2225	U, wdir, T, RH, p	R. M. Young 05103/61201 (U, wdir, p); Rotronic TM12R (T, RH)	1
2236	U, wdir, T, RH, R _{sd} , p	Davis Energy Enviromonitor	10
2134	T	Crossbow MTS300CA	.2
1989	T, RH, U, wdir	Vaisala HMP35C, Davis wind	5
1910	T	Crossbow MTS300CA	.2
1795	T, RH at 1.6 & 7.6 m, turbulent fluxes, 3D-wind, R _{net}	Vaisala HMP35C, CSAT3, REBS Q7, Davis wind	5
1641	T	Crossbow MTS300CA	.2
1435	T	Crossbow MTS300CA	.2
26	U, wdir, T, RH, R _{sd} , p	Davis Energy Enviromonitor	10

^aThe station at 2225 m is the PICO-NARE observatory. Avg, averaging time; wdir, wind direction; U, wind speed; T, temperature; RH, relative humidity; p, pressure; R_{sd}, downwelling shortwave radiation; R_{net}, net radiation; CSAT3, three dimensional Campbell Scientific sonic anemometer-thermometer; MSL, mean sea level.

locations shown in Figure 1b. Seven of these stations were located along a line extending down the western slope of the mountain; the eighth was located at sea level to the south. The meteorological measurements at each station are summarized in Table 1.

[26] All stations included temperature measurements at ~ 1.6 m above ground level (AGL). Crossbow Mica2 wireless sensor network motes with Crossbow MTS300CA sensor boards mounted inside radiation shields were used as a cost-effective and lightweight way of measuring temperature at four of the stations (those at 1435, 1641, 1910, and 2134 m). Since sleep modes were not employed, battery life (using 2 AA batteries) was only 2–6 days, which caused extended downtimes at these stations. (For the analyses of mean diurnal cycles presented below, only stations with at least 4 days or 96 hours of data are included.) Relative humidity (RH) and wind measurements were also made at four stations (those at 26, 1795, 1989, and 2236 m). RH sensors were colocated with the temperature sensors, while anemometers were mounted at ~ 2.7 m AGL. The exception to this rule was the sonic anemometer (Campbell Scientific, CSAT3) at the 1795 m station, which was mounted at 4.2 m AGL in a true vertical position. All temperature, relative humidity, and pressure sensors were intercompared at the beginning and the end of the experiment and were found to operate within their specifications ($\Delta T < 0.5$ K, $\Delta RH < 3\%$, $\Delta p < 1.7$ hPa or better).

[27] To compute turbulent momentum fluxes from the CSAT3, the coordinates were rotated such that the average vertical velocity was zero [Wilczak *et al.*, 2001]. To compute potential temperature, atmospheric pressure at stations without pressure sensors was obtained by polytropic pressure adjustment from the nearest station including pressure measurements, according to

$$p_2 = p_1 \left(\frac{T_{v2}}{T_{v1}} \right)^{g/R\gamma_v}, \quad (4)$$

where g is the gravitational constant, R is the gas constant for dry air, and γ_v is the vertical virtual temperature gradient. For T_{v1}, T_{v2} and γ_v , data from ECMWF profiles were used (see section 2.3).

2.3. Soundings

[28] Vertical soundings were obtained for use in the estimation of mechanically forced lifting and for comparison of conditions on Pico mountain to those over the surrounding ocean. Vertical profiles of temperature, dew point temperature, wind speed, and wind direction were obtained from radiosoundings from Terceira Island (38.73°N , 27.07°W) (<http://raob.fsl.noaa.gov>, accessed 25 July 2005) and from the ECMWF global numerical weather model (0.5° latitude-longitude resolution, 6 hourly, <http://www.ecmwf.int>, accessed during December 2005). Unfortunately, there is only one Terceira sounding per day in the summer, and the release location is displaced from the Pico mountain by 119 km. For this reason, the ECMWF profiles, although at a coarse vertical resolution, are expected to be more representative of the atmospheric conditions at Pico. (The radiosonde data from Terceira are assimilated into ECMWF, however.) We used the ECMWF reanalysis data

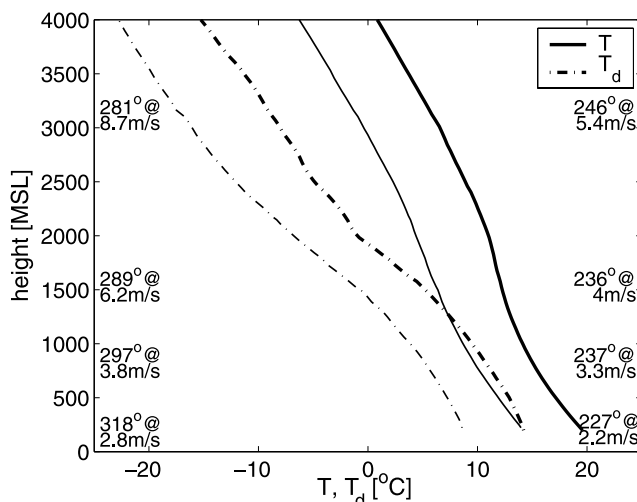


Figure 2. Mean soundings of temperature T and dew point temperature T_d over the island of Terceira (38.73°N , 27.07°W) for summer (June–August, thick lines) and winter (December–February) from 1999 to 2004. Average wind vectors at 1000, 925, 850, and 700 mbar are given on the left for winter and on the right for summer at the corresponding elevations in meters.

set (ERA40) until August 2002, and the operational model (T511) thereafter. The soundings used below are based on ECMWF data from 18 pressure levels between the surface and 700 hPa, horizontally interpolated to the location of Pico mountain from the four surrounding numerical grid points.

3. Local and Regional Environment of the PICO-NARE Station

[29] Pico Island, the site of the PICO-NARE station, is quite small, approximately 45 km long and 15 km wide, resulting in overland fetches upwind of the station of 7–13 km for the most common wind directions, between southwest and north. Total island population in 2004 was 14,729 [*Serviço Regional de Estatística dos Açores*, 2005] (accessed May 2006), and the nearest road ends at an elevation of 1250 m, 970 m below and 2 km south-southwest of the station.

[30] The Azores Islands are located in the central North Atlantic Ocean. The climate in this region is strongly influenced by the strength and location of the Azores High. During summer, a strong, stationary Azores High frequently causes weak winds and enhanced large-scale subsidence [*Hastenrath and Greischar*, 2001]. During winter, the high is typically located further to the south, causing cyclones with strong westerly winds to pass over the island. These seasonal changes also affect the mean boundary layer structure. Figure 2 shows mean winter and summer profiles of wind speed and direction, temperature, and dew point temperature obtained from radiosoundings on the nearby island of Terceira (119 km distant).

[31] During winter, the winds above 1000 m are approximately 50% stronger than during summer and are predominantly from the west to west-northwest, while summertime

winds are on average from the west-southwest, reflecting the changing location and strength of the Azores High. Because of the maritime location, differences between summer and winter temperatures are small: approximately 5 K at 500 m MSL, increasing to 6.5 K at 2000 m MSL. This increase in the seasonal temperature difference with height is the result of seasonal differences in the inversion height, which is lower during summer, presumably because of enhanced subsidence associated with the stronger Azores High in that season.

[32] The seasonal variation of the MBL height (i.e., the height of the bottom of the capping inversion) is shown by the solid line in Figure 3. MBL heights shown in Figure 3 were obtained from the final run (FNL) of the GDAS global numerical weather model (1° latitude-longitude resolution, 6 hourly, obtained through HYSPLIT output [Draxler and Rolph, 2003]) over the period July 2001 to August 2005. (MBL heights were also estimated from the Terceira radiosoundings; these exhibit a similar seasonal cycle.) Reduced MBL heights (850–1100 m on average) are present during May–September. During October–April, the MBL is deeper, typically between 900–1700 m, but remains lower than the height of Pico mountain.

4. Mechanically Forced Upslope Flow

[33] Dividing streamline heights (z_t) were calculated using equation (2), with wind speed and Brunt-Vaisala frequency N obtained from the ECMWF profiles. The resulting values indicate the minimum origin elevation of air traveling over the mountaintop and are summarized in Figure 3 (dashed line). z_t exhibits an annual cycle that is opposite that of MBL height. During winter, the higher wind speeds and reduced stability in the lower atmosphere result in lower values of z_t , that is, a greater degree of mechanically forced uplift, while lower winds and a more stable lower FT during summer result in less uplift and larger z_t .

[34] The dividing streamline height may be compared to the MBL height to identify periods in which MBL air may have reached the station. During the months of May to September, the interquartile ranges of MBL heights shown in Figure 3 do not overlap with the interquartile range of z_t . This implies that it is unusual for mechanically forced lifting to bring MBL air to the summit station during summer. In contrast, the MBL is higher and z_t is lower during the rest of the year. As a result, there is considerable overlap between the distributions of the two variables. The fraction of each month during which z_t was less than the MBL height is listed at the bottom of Figure 3. On the basis of the July 2001 to August 2005 period analyzed here, the probability of potential MBL impact due to mechanically forced upslope flow ranges from a low of 4% in July to a maximum of 59% in March.

[35] We have evaluated the accuracy of these z_t calculations by using them to predict the occurrence of orographic clouds at Pico summit. In this analysis, presented elsewhere [Kleissl et al., 2006], temperature and humidity at z_t were used to determine whether condensation would occur if air was lifted from z_t to the summit. The predictions were evaluated using relative humidity measurements at the PICO-NARE station, with the presence of clouds indicated

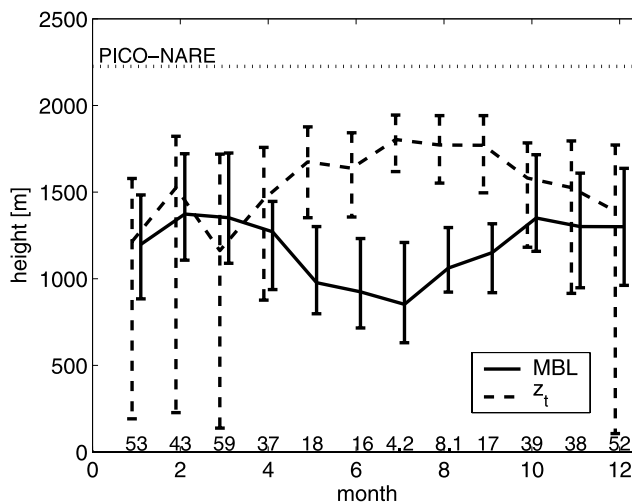


Figure 3. Mean and interquartile range of marine boundary layer height (MBL) and dividing streamline height (z_t) for the period July 2001 to August 2005 as a function of month of year. The numbers at the bottom give the percent fraction of times when $z_t < \text{MBL}$, i.e., the likelihood of MBL air reaching the station for a given month.

by RH values above 98%. The model predictions were correct more than 85% of the time. Comparisons of specific humidity and potential temperature at the PICO-NARE station with corresponding ECMWF values at z_t suggested that Sheppard's model underpredicts the amount of uplift for weak wind speeds, but predicts the relative increase in uplift with increasing U_∞/Nh correctly. More than 50% of the incorrect predictions could be explained by z_t errors of less than 210 m.

[36] Two additional tests of the adequacy of the mechanical uplift estimates were possible during summer 2004: an evaluation of the wind direction and temperature profile along the meteorological stations mounted on the west side of the mountain, and a comparison of measurements at the PICO-NARE station to soundings obtained by the FAAM BAe-146 aircraft during the ITOP study.

[37] By analyzing wind directions at the mountainside meteorological stations during mechanically forced upslope flow periods, we found that upslope flow along the western side of the mountain only resulted when synoptic winds were from the west-northwest. Slight deviations from west-northwest in the incoming flow resulted in nearly horizontal flow at the meteorological stations on the western slope. Since Pico is a nearly symmetric mountain, this implies that upslope flow capable of reaching the summit is limited to a narrow sector on the upwind slope of the mountain.

[38] During summer 2004, there were five periods of moderately strong upslope flow ($z_t < 1700$ m) during which synoptic winds were from the west-northwest (ECMWF wind direction at the dividing streamline height equal to 270–305°), four or more mountainside temperature measurements were available, and meteorological conditions were consistent for at least one hour. These periods are shown in Table 2. Four of these periods resulted in water vapor saturation on the mountainside. During uplift from z_t

Table 2. Conditions During Five Periods of Moderate Mechanically Forced Upslope Flow During Summer 2004

Time, UTC	ECMWF				1795 m Station		LR, ^a K km ⁻¹	Adiabatic LR ^b
	wdir(z_t), deg	$U(z_t)$, m s ⁻¹	z_t , m	FNL, MBL, m	wdir, deg	U , m s ⁻¹		
5 Aug, 1300–1800	278	12.7	1328	712	216	4.02	-4.7 ± 1.9	-4.8
7 Aug, 0126–0325	304	12.8	1187	497	282	5.23	-5.3 ± 1.2	-5.0
16 Aug, 0900–1700	277	12.1	739	1510	245	7.43	-5.5 ± 0.7	-5.0
21 Aug, 2300 to 22 Aug, 0400	282	11.7	1695	1095	258	4.86	-4.9 ± 0.9	-4.9
22 Aug, 1400–1500	293	8.43	1650	1232	268	3.78	-8.4 ± 3.9	(-9.7)

^aLR, lapse rate. Observed LRs are calculated using least-squares regression of observations above elevation z_t .

^bMoist adiabatic LRs are calculated for 5–21 August; the dry adiabatic LR is shown for 22 August, 1400–1500 UTC.

to the summit under the low-insolation conditions typical of mechanical lifting periods, temperature profiles during these four events should follow the moist adiabatic lapse rate, while that during the dry event should follow the dry adiabatic lapse rate. As shown in Table 2, observed lapse rates were consistent with these expectations.

[39] During mid-July to mid-August 2004, the ITOP mission was based on the island of Horta, adjacent to Pico island, and the FAAM BAe-146 aircraft obtained profiles around Pico mountain on 4 days [Lewis *et al.*, 2006]. These aircraft measurements provide an additional method for evaluation of the elevation of air sampled at the PICO-NARE station. The aircraft measurements of O₃ and potential temperature on 31 July and 1 August 2004, are shown in Figure 4. The potential temperature profiles indicate a nearly neutral marine boundary layer capped by a stable region extending from approximately 1000 m to above

2500 m on both days. The O₃ profiles on these 2 days were significantly different. On 31 July (Figure 4a), low O₃ levels were present above 1700 m, but a layer of enhanced O₃ was sampled by the aircraft just above the boundary layer. In contrast, on 1 August (Figure 4b), multiple layers with varying O₃ levels were present in the lower FT, all with greater mixing ratios than in the MBL. On both days, the PICO-NARE measurements were consistent with the sampling of air between z_t and the actual station elevation, but were not consistent with sampling of air from the region below z_t . Vertical soundings near Pico were obtained on 2 additional days (not shown). O₃ and CO measurements at the PICO-NARE station were consistent with ITOP measurements between z_t and station elevation on each of these days as well.

[40] In summary, mechanically forced uplift on Pico mountain is most important during October through April.

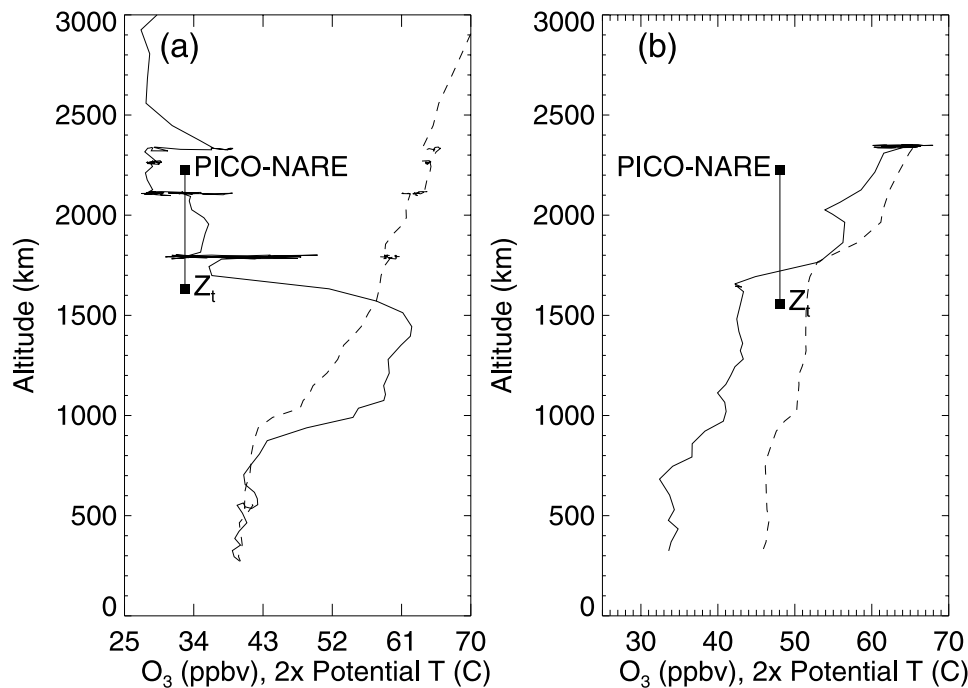


Figure 4. O₃ (solid) and potential temperature (dashed) profiles and simultaneous PICO-NARE O₃ observations (boxes) on (a) 31 July 2004, 1442–1512 UTC, and (b) 1 August 2004, 1401–1413 UTC. O₃ and potential temperature profiles were obtained by the FAAM BAe-146 aircraft within 25 km of Pico summit. The 30-min-average PICO-NARE O₃ measurement centered on the midpoint of the flyby is plotted twice in each figure: at the elevation of the PICO-NARE station and at the dividing streamline height, z_t . The line drawn between these two heights emphasizes the region of possible origin of the air sampled at the PICO-NARE station at each time.

During this period, our calculations indicate that upslope flow strong enough to carry MBL air to station elevation occurs 37–59% of the time. In contrast, mechanically forced upslope flow is weaker during May through September. In particular, we estimate that it carries MBL air to station elevation less than 20% of the time during this period. Since air may diverge around Pico mountain as it rises over it, or may mix with higher-altitude air of a composition that is poorly constrained as a function of altitude, it is difficult to estimate the degree of mixing during uplift or to quantify the uncertainty in the z_t calculations. However, evaluations using observations of mountaintop clouds and using vertical soundings during the ITOP study indicate that the calculated degree of uplift provides a reasonable upper limit that should be useful for identification of periods when mechanically forced uplift of MBL air does not impact station measurements.

5. Buoyant Upslope Flow

5.1. Frequency During Summer 2004

[41] The conditions required for buoyant upslope flow (BUF), strong solar heating and low or moderate synoptic winds, often occur on Pico Island during summertime, as a result of the presence of the Azores High. On the western slope, where our meteorological measurements were made, nighttime downslope flow results in easterly horizontal winds and a negative vertical wind speed w , while daytime upslope flow results in westerly horizontal winds and a positive w . The w measurements by the 3D sonic anemometer (CSAT3) can provide more accurate measurements of the upslope flow velocity than can the horizontal wind speed and direction, but occasional supersaturated conditions (due to buoyant or mechanical upslope flow) caused condensation and malfunction of the sensor. These discontinuities in the data prevented us from using it as the primary selection criterion for BUF days.

[42] Days on which significant BUF occurred were identified on the basis of shifts in mean wind direction at the 1795 m station on the western slope between daytime and nighttime as follows: upslope flow with wind direction between 225 and 315° during daytime (1200–1800 UTC) surrounded by downslope flow with wind directions between 0 and 180° between 0400–0600 and 2300–0100 UTC. (All times in this paper are UTC. UTC is equivalent to local daylight savings time, LDST, or Azorean Summer Time, and lags solar time by 2 hours.) On the basis of these criteria we identified 14 days with BUF. Days that were not selected because they did not satisfy one of the two nighttime downslope criteria were inspected individually to determine whether daytime upslope flow may have occurred despite the lack of downslope flow at morning or evening. One such day was found: on 17 July, strong mechanical uplift prior to noon prevented early morning downslope flow. The period 17 July, 1200–2400 UTC was therefore added to the set of BUF days, resulting in a total of 15 days with BUF.

[43] Since it is possible that BUF in the presence of moderate synoptic winds not from the west could result in a daytime wind direction that did not satisfy the upslope flow criterion, we also inspected all non-BUF days on which daytime-average vertical wind speeds measured by

the CSAT3 at 1795 m exceeded 0.6 m s^{-1} . Fifteen such days were found. Three of these additional days were among those identified above as days on which mechanically driven uplift was strong enough to carry MBL air to the summit, and four more occurred on days when mechanically driven uplift was present at the CSAT3 station ($z_t < 1700 \text{ m}$), but too weak to carry MBL air to the summit. This apparently caused the observed positive vertical velocities that did not follow insolation. The remaining eight periods appeared to be the result of buoyant forcing in the presence of moderate synoptic winds (buoyant plus mechanical forcing, termed “B&M”). On such days no orographic clouds were observed at the summit (contrary to expectations for stronger mechanically forced uplift). The wind vector typically had a downslope component at night and an upslope component during the day, but the buoyant forcing was not strong enough to align the wind vector with the slope enough to satisfy the BUF criterion, i.e., the flow was more horizontal. On B&M days the wind direction is expected to be aligned with the slope only on the aspect of the mountain facing the wind. On this aspect the buoyant forcing will be aligned with the mechanical forcing during daytime, thus creating an effective dividing streamline height that is lower than the one calculated for mechanical lifting alone. On other sides of the mountain, horizontal wind speeds will be larger than vertical wind speeds, leading to wind vectors directed at a shallow angle around the mountain, preventing buoyant uplift over any significant elevation range.

[44] Finally we also inspected days during which the daytime wind direction was from the west (180°–360°) and the CSAT3 was not operating properly because of condensing water. Out of 10 such days, 9 were associated with strong mechanical upslope flow ($z_t < 1550 \text{ m}$) resulting in formation of thick orographic clouds which prevented strong buoyant forcing. One day with only intermittent cloud cover and weaker mechanical forcing (4 August) was included in the B&M data set.

[45] The 15 BUF days plus 9 B&M days constitute 39% of the number of days in the study period. Considering that buoyant forcing typically occurred for 10 hours per BUF or B&M day, 16% of the summertime measurements at the PICO-NARE station were potentially influenced by buoyant upslope flow. In 2004, most of the BUF and B&M events occurred during late June and July; only 1 BUF day and 2 B&M days were identified in August. However, in 2005 isoprene (a tracer from lower elevations with vegetation, see section 5.4) was observed mostly in August. Since the amount of mechanical forcing is weakest in July and August (largest z_t in Figure 3) and the solar zenith angle is smallest from May–August, on average most of the buoyant forcing events are expected to occur in July and August.

[46] As discussed above, our selection criteria for BUF are based on the wind direction and checked using w measurements that are unavailable during periods when surface clouds were present at the CSAT3. It is thus possible that weak BUF on days with significant synoptic winds may have occurred on other days not identified here. However, the strength of BUF on such days is expected to be less than on the days identified here, since the presence of clouds reduces the solar forcing consistent with the absence of a wind direction shift.

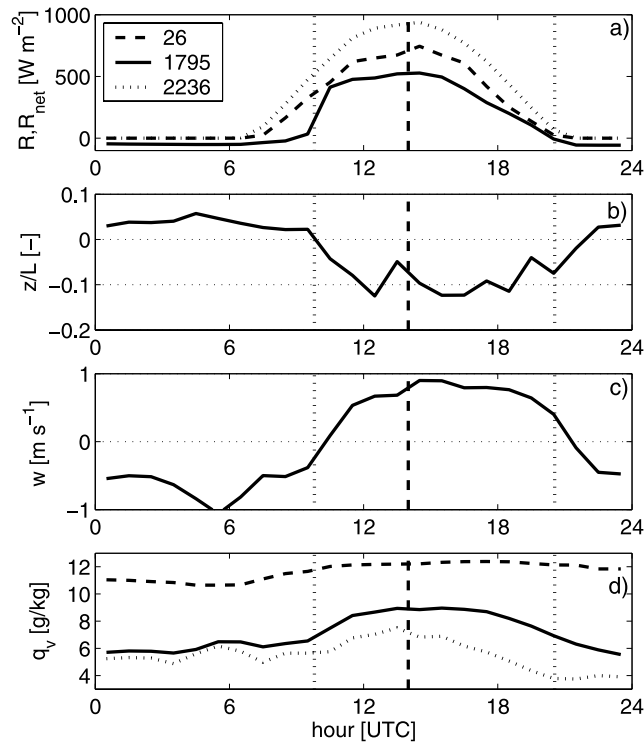


Figure 5. Mean daily evolution of meteorological variables during BUF days. Vertical dotted lines show average sunrise and sunset and the vertical dashed lines show solar noon (1400 UTC) at the station at 1795 m. UTC is equal to local (Azores) daylight savings time. (a) Solar radiation R . At the 1795 m station, the net radiation R_{net} is depicted. (b) Atmospheric stability z/L , (c) vertical velocity w , and (d) specific humidity q_v .

[47] Upslope flow (westerly wind) on BUF days typically occurred between approximately 1000 and 2100 UTC. The overall average vertical wind speed and direction at the 1795 m station during these periods were 0.70 m s^{-1} and 278° , respectively. The largest daily average was 0.83 m s^{-1} and the largest 10 min average was 1.83 m s^{-1} . At these vertical wind speeds, the time required to travel the entire altitude of Pico mountain would be less than one hour. However, the degree to which low-elevation air actually impacted the summit station is evaluated below.

5.2. Mean Diurnal Evolution

[48] The mean diurnal variation of meteorological variables characteristic of upslope flow provides additional insight into these periods. Figure 5 shows the mean diurnal variation of solar radiation, atmospheric surface layer stability z/L (height divided by the Monin-Obukhov length) derived from the CSAT3, vertical wind speed, and specific humidity. Daytime insolation and nighttime radiative cooling are the driving forces of buoyant flows. At night, the net radiation measured at the 1795 m station was negative (-54 W m^{-2} on average between 2130 and 0630 UTC), as a result of radiative cooling of the ground (Figure 5a). Sunrise was first observed at the mountaintop station (2236 m) at 0655 UTC, then at the near-sea-level (26 m) station on the south side of the island at 0720 UTC, while

the mountain obstructed insolation on the western slope until 0948 UTC. During the day, the mountaintop insolation varied smoothly with time, indicating cloud-free conditions, while incoming radiation at the 1795 m and 26 m stations was reduced by orographic clouds. At all stations, maximum insolation occurred around local solar noon at 1400 UTC. (Sunrise, solar noon, and sunset at the 1795 m station are indicated on Figures 5 and 6.)

[49] Solar forcing influences the stability parameter z/L (Figure 5b). At night, z/L was positive, that is, stable atmospheric conditions were observed ($z/L = 0.04$ on average). After sunrise, large sensible heat fluxes over the lava rock in combination with low wind speeds in the buoyant flows resulted in moderately unstable conditions with negative z/L . Unstable conditions persisted until more than an hour after sunset.

[50] The most important indicator of upslope or downslope flow is the vertical wind speed w (Figure 5c). Downslope flow (negative w) occurred at night, with speeds around -0.5 m/s . Shortly after sunrise, w became positive, and the average w remained large ($\sim 0.8 \text{ m s}^{-1}$) and fairly constant between 1200 and 1900 UTC.

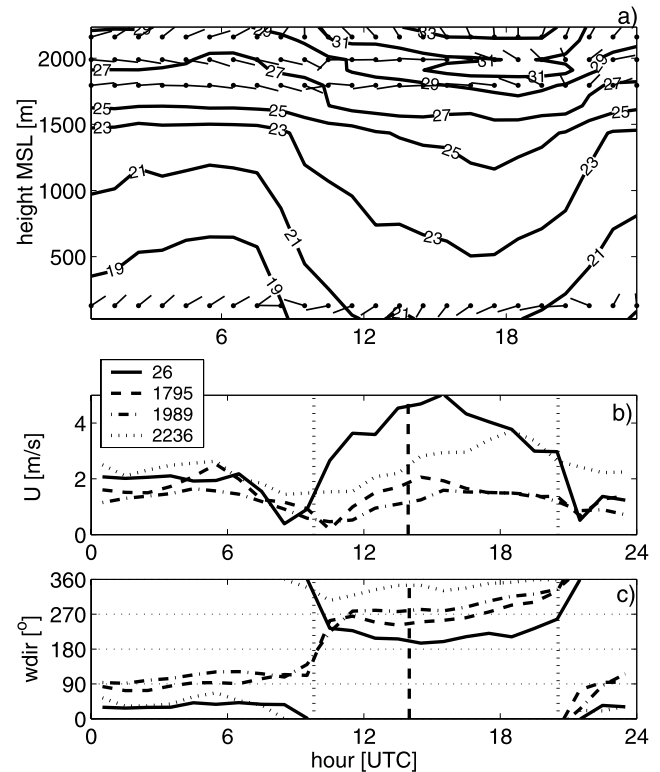


Figure 6. Mean daily evolution of potential temperature, wind speed and wind direction during BUF days from the measurements described in Table 1. Vertical dotted lines show average sunrise and sunset and the vertical dashed lines show solar noon (1400 UTC) at the station at 1795 m. UTC is equal to local (Azores) daylight savings time. (a) Contour plot of potential temperature θ in $^\circ\text{C}$ with direction of mean wind vector. (b) Mean resulting horizontal wind speed. (c) Mean wind direction (computed like direction of mean wind vector but assuming constant wind speed).

[51] Specific humidity, which is conserved during uplift in the absence of condensation or evaporation of water from the soil, may be used to characterize the degree of uplift along the mountain slope. Figure 5d shows specific humidity at three stations. During daytime when clouds were frequently observed at the 1795 m station, the q_v values shown in Figure 5d are lower than the total humidity ($q_v + q_l$) at that station. In contrast, since clouds were rare at the 2236 m station the total humidity there is not expected to be significantly different from the specific humidity q_v . Evapotranspiration could also affect q_v , but is expected to be insignificant, as a result of the near absence of vegetation and the rocky surface.

[52] During night, when downslope flow may bring dry air to the upper stations, the station near sea level measured the largest q_v , and the summit station measured the lowest. During daytime, q_v increased significantly at all mountain stations, indicating that upslope flow brought air originating at lower elevations to these stations. However, q_v remained significantly lower at the mountainside stations, and much lower at the summit station. Since clouds were rare at the summit station, the lower q_v at the summit station implies that air was not lifted from 1795 m directly to the summit station. Instead, mixing with higher-altitude air, possibly in combination with partial flow around the mountain, must have occurred during buoyant uplift occurred. Drier conditions at the summit are also apparent in MODIS true-color images taken during the afternoons of BUF days. In each case, a cloud-free region is visible over part or all of the summit caldera.

[53] The evolution and timing of upslope flow and its effect on slopewise stability can be best visualized using the plots of potential temperature contours, wind speed, and wind direction shown in Figure 6. On BUF days, the wind direction (Figure 6c) at the stations on the slope (1795 m and 1989 m) shifted sharply 180° from downslope (easterly) to upslope (westerly) within one hour after sunrise (0930–1030 UTC). This shift was accompanied by a brief period of calm winds (Figure 6b). At the mountaintop (2236 m) station, the wind direction shift was much more moderate, shifting from northeast at night to northwest during the daytime. The mountaintop station is more exposed to the synoptic flow field which, though it was weak on these BUF days, nevertheless significantly altered the buoyancy driven flow. The significant alteration in the wind direction near the summit implies that air lifted toward the summit is blown around the mountain as it rises, and suggests that air ascending the mountain on the upwind flank may have the greatest chance of impacting measurements on the summit.

[54] Nocturnal cooling and daytime heating of the slope can be identified in the mean potential temperature contours shown in Figure 6a as a function of elevation and time of day. A stable temperature gradient is present along the mountain slope during both night and day. This stable structure must reduce the ability of upslope flows to travel continuously up the mountainside. For example, to rise from the typical MBL height of 1000 m to the summit at midday, the rising air would need to overcome a potential temperature increase of approximately 9 K. Even at a relatively low (for BUF days) midday vertical velocity of 0.5 m s^{-1} , this would require a 16 K hr^{-1} heating rate, which is unrealistically high (e.g., compare the heating rate over

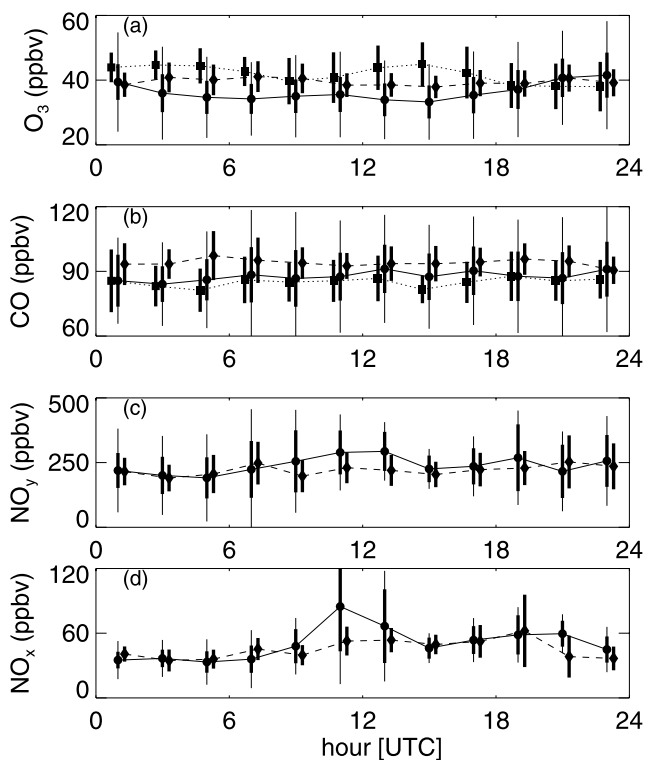


Figure 7. Mean daily evolution of (a) O_3 , (b) CO , (c) NO_y , and (d) NO_x mixing ratios at the PICO-NARE station during BUF days (solid lines), B&M days (dotted lines), and non-upslope days (dashed lines). Measurements are not available during all days, and only 2-hour bins containing at least 8 hourly average measurements are shown. For NO_x and NO_y , this prevents the assessment of diurnal cycles during the B&M days. Circles indicate the mean value of all hourly average measurements in each 2-hour bin, thick vertical lines extend ± 2 standard errors of the mean, and thin vertical lines extend ± 1 standard deviation of the measurements in each bin. (For clarity, standard deviations are shown only for the BUF data.) Non-upslope days exclude days identified as BUF, mechanically driven upslope, or a combination of the two. UTC is equal to local (Azores) daylight savings time and lags solar time by 0200 hours.

the lava surface on Hawaii Island: $\sim 1.7 \text{ K hr}^{-1}$ [Mendonca, 1969]). Thus we conclude that it is unlikely that air from within the MBL regularly rises directly to the summit on these days.

5.3. Impacts on PICO-NARE Atmospheric Chemistry Observations

[55] Chemical measurements at the PICO-NARE station provide an alternative indicator of the degree to which air from lower elevations may have reached the station. If air from the populated regions of the island reached the station during BUF periods, afternoon enhancements in anthropogenically emitted trace gases, e.g., CO , nitrogen oxides, and hydrocarbons would be expected. Alternatively, if clean MBL air were sampled, reductions in NO_y [Peterson et al., 1998] and O_3 [Oltmans et al., 1996] would be expected on average, although the vertical distribution below 3 km is variable, as shown in Figure 4 above.

[56] Figure 7 shows the diurnal variations of O_3 , CO, NO_y , and NO_x during BUF days, B&M days, and non-upslope flow days. No diurnal cycle is detectable for O_3 or CO in any data subset. For the BUF days, on which a diurnal cycle would be expected if MBL air were carried to the station, the day-minus-night difference for O_3 is 0.0 ± 3.5 ppbv, and for CO it is 1.7 ± 7.3 ppbv (differences are between nighttime, 2230–0930 UTC, and daytime, 1030–2030 UTC, averages, ± 2 standard errors of the difference). For the nitrogen oxides, there is an indication of higher midday NO_y levels during BUF days, but the day-minus-night difference on those days is not significant (38 ± 52 pptv). However, the midday increase in NO_x is significant (25 ± 14 pptv). Most of this NO_x difference is the result of measurements on 1 day: 5 July.

[57] On 5 July the lower atmosphere was weakly stable up to 1900 m and a strong capping inversion present in the sounding between 2100 and 2350 m, with very dry air aloft. Prior to the onset of BUF on this day, the specific humidity observed on the mountain exhibited the typical stratification of drier air aloft. However, between 1100 and 1630 UTC the specific humidity and O_3 showed frequent positive and negative (up to 16 ppbv) excursions, respectively, indicating transport of subinversion air to the PICO-NARE station. Despite significant increases throughout the day, the upper limit of q_v remained significantly below that at the 1795 m station, in absence of persistent clouds.

[58] Coincident with the first increase in q_v , a large spike in NO_x was observed, reaching approximately 1000 pptv, an increase of more than an order of magnitude. Since the NO_x enhancement was only observed during a brief episode of westerly winds and coincided with a spike in CO of 122 ppbv, it may have been caused by the station diesel generator, located at 1250 m MSL on the western slope of the mountain.

[59] These observations on 5 July demonstrate that uplift of air over a vertical distance of 1 km or more and from within the MBL can potentially occur during some BUF events. However, this was the only day on which variations in trace gas mixing ratios could be unambiguously attributed to buoyant uplift from below the MBL height. Negative correlations between O_3 and q_v and elevated q_v during daytime were present during portions of several other BUF or B&M days (1, 18, and 20 July). However, nitrogen oxides measurements, available on 11 of these days, did not exhibit corresponding enhancements. Since q_v - O_3 anticorrelation was also common to non-upslope flow days and was observed during both day and night, it is probable that this anticorrelation results from lower FT layering rather than the sampling of air of MBL origin.

5.4. Hydrocarbon Measurements in 2005 and Detection of BUF Episodes

[60] During summers when mountainside meteorological measurements are not available, periods of potential BUF need to be identified on the basis of data from the PICO-NARE station or from numerical weather prediction models. Since October 2004, NMHC have been routinely monitored using a gas-chromatography system [Tanner *et al.*, 2006]. Besides monitoring of long-lived C_2 – C_6 NMHC,

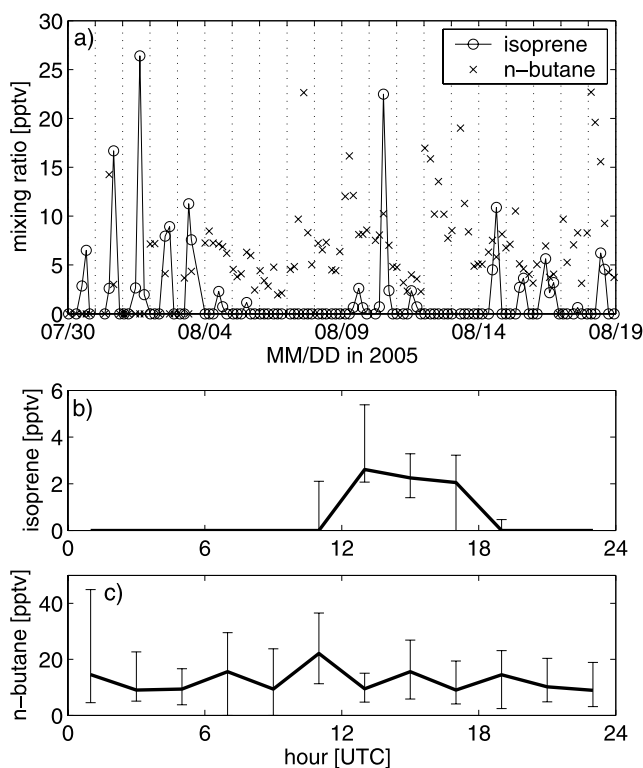


Figure 8. NMHC data from the PICO-NARE station. (a) Time series of n -butane and isoprene during the period 30 July to 19 August 2005. Composite diurnal cycle of (b) isoprene and (c) n -butane on days during January–August 2005 when daily maximum isoprene exceeded 1 pptv. The line connects medians of measurements in each 2-hour bin, and error bars extend from the lower to the upper quartile. UTC is equal to local (Azores) daylight savings time and lags solar time by 0200 hours.

these measurements also capture isoprene, an unsaturated and short-lived hydrocarbon (summertime atmospheric lifetime is <1 hour) emitted mostly from broadleaf vegetation as a byproduct of photosynthesis. Isoprene is emitted instantaneously, therefore emissions occur only during daytime hours and cease during the night. Because of the near-absence of vegetation near the mountaintop, isoprene is presumably transported from lower elevations (less than ~ 1500 m) to the PICO-NARE station by upslope flow. Given its short lifetime, transport from other landmasses than Pico itself can be excluded. Figure 8a shows a typical time series of isoprene mixing ratios at the station during three weeks of August 2005. Striking features are the highly variable and large increases of isoprene during daytime hours. Isoprene at the station during this period showed large variations with daytime maximum mixing ratios ranging from less than 1 pptv to 26 pptv. Isoprene was detected on 54% of the shown days, and exceeded 1 pptv on 44% of all days (with available data) from May–August 2005. The diurnal cycle of isoprene occurrences is further analyzed in Figure 8b, which includes measurements from all days on which isoprene >1 pptv was detected. The largest isoprene mixing ratios are found between 1200 and 1800 UTC, corresponding to the time of strongest

BUF (Figure 5). More than 75% of isoprene observations before 1000 UTC and after 2000 UTC were <1 pptv, consistent with the downslope flow observed at the meteorological stations in summer 2004.

[61] Figure 8a also includes measurements of *n*-butane, and the composite diurnal cycle of *n*-butane on days when isoprene exceeded 1 pptv is shown in Figure 8c. In contrast to isoprene, *n*-butane does not exhibit a diurnal cycle. *N*-butane has a much longer atmospheric lifetime (~ 44 hours in summer) and has mainly anthropogenic sources. *N*-butane is an abundantly used energy source for domestic heating and cooking on Pico Island. These facts make this compound a sensitive indicator for the influence of local anthropogenic emissions.

[62] Unfortunately concurrent *n*-butane measurements from lower island elevations for comparison with the station data are not available. However, NMHC measurements from the adjacent island Terceira made during the 1993 NARE experiment [Fehsenfeld *et al.*, 1996] allow further, qualitative interpretation of the PICO-NARE data. The Terceira data showed that NMHC levels at the 1010 m Santa Barbara mountain (which is the highest mountain on Terceira Island, but, in contrast to Pico Mountain, expected to be much more exposed to MBL air) were low compared to four other Atlantic data sets, but a variability analysis indicated that NMHC were notably influenced by local emissions [Jobson *et al.*, 1998]. For 114 samples collected during 3 August to 2 September 1993, median mixing ratios were 817 pptv for ethane, 80 pptv for propane, and 22 pptv for *n*-butane. During August of 2005, median mixing ratios at the PICO-NARE station were 601 pptv for ethane, 40 pptv for propane and 5.8 pptv for *n*-butane, which are all lower than the Terceira 1993 values.

[63] Daytime increases in *n*-butane, especially if correlated with increases in isoprene, would indicate BUF or B&M from populated areas, which on Pico Island are mostly located near sea level. However, no such daytime increase in *n*-butane is evident in the diurnal cycle shown in Figure 8c. In addition, we examined the most pronounced isoprene events on a case-by-case basis: no strong corresponding increases in *n*-butane were observed. Conclusively, the lower, absolute levels at PICO-NARE, the lower variability in the *n*-butane data and the fact (Figure 8c) that no *n*-butane enhancements are discernable even during times when isoprene measurements imply BUF conditions, all suggest that BUF does not transport air from sea level to the PICO-NARE station, but that the BUF air most likely originates at higher elevations.

[64] When isoprene measurements are available, they offer the most reliable (tracer-based) identification of BUF and daytime B&M conditions at the PICO-NARE station, although the minimum height from which air is lifted on these days is not yet known and may be as little as 700 m below station elevation. When isoprene measurements and mountainside meteorological measurements are not available (as was the case 2001–2003), numerical weather model data can be used to identify days with buoyant forcing.

[65] Meteorological parameters from numerical weather model data which determine the strength of BUF are the downwelling shortwave radiation at the surface (dswf) and the horizontal wind speed. In Figure 9 we identify that

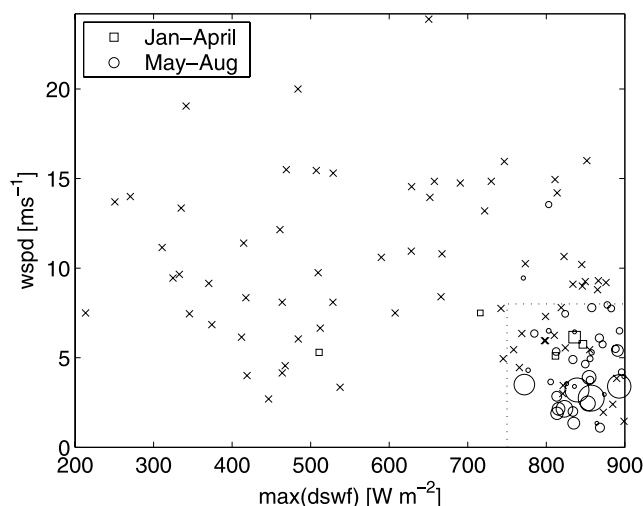


Figure 9. Scatterplot of maximum daily downwelling shortwave radiation (dswf) at the surface from FNL data and averaged daytime horizontal wind speed near 850 hPa from ECMWF, on days when isoprene was detected during January–April (squares) and May–August 2005 (circles) and on days when no isoprene was observed (crosses). For squares and circles, the area of the symbol is proportional to the maximum daily isoprene concentration observed. The largest circle has an area corresponding to 26 pptv of isoprene. The dotted lines show the recommended screens to predict BUF or B&M days on the basis of dswf and wind data.

isoprene episodes mostly occur on days with low synoptic wind speeds (e.g., ECMWF 850 hPa wind speed less than 8 m s^{-1}) and summer days without cloud cover (e.g., FNL dswf at noon larger than 750 W m^{-2}). During January–August 2005, these rules would have predicted 85% of the isoprene events (and all of the events with isoprene mixing ratios >2.7 pptv) while erring on 24% of the nonisoprene events. In summer 2004, these rules would have detected 91% of the BUF and B&M days while erring on 31% of the non-BUF and non-B&M days.

[66] Figure 9 shows few isoprene observations under the high wind conditions that lead to mechanically driven upslope flow. The absence of isoprene in strong winds might be caused by reduced isoprene emission rates on these days due to lower temperatures and attenuation of solar radiation under conditions of thick orographic clouds (a process not captured by the FNL dswf product because of its coarse resolution), as well as by greater dilution resulting from increased mixing in stronger winds. In addition, mechanical lifting is not expected to be as effective as BUF in transporting near-mountain air to the mountaintop, since the dividing streamline only slowly converges to the mountain surface as it approaches the mountaintop.

6. Summary and Conclusions

[67] We have characterized upslope flow on Pico mountain using a 3.5 year climatology of mechanically forced lifting, intensive meteorological measurements conducted during summer 2004, and chemical measurements during 2004–2005 for the purpose of assessing the occurrence of

mechanically forced and buoyant upslope flow (BUF). Measurements at the PICO-NARE station are affected by both types of flows, with mechanically driven uplift dominating during winter and buoyant uplift during the summer. Our analysis indicates that on most days FT air is sampled at the station throughout the day. During the 62-day summer 2004 intensive period, mechanically driven and BUF, together, occurred 25% of the time during portions of 50% of the days studied. Impacts of marine boundary layer (MBL) air at the station were detected on only a fraction of these days.

[68] Mechanically forced upslope flow is most important during October through April, when it is strong enough to carry air from the MBL to the summit 35–60% of the time. In contrast, lower synoptic wind speeds and a more stable lower FT result in much lower probabilities (<20%) of MBL impacts due to mechanically forced upslope flow during May–September. During periods when the dividing streamline height z_t is within the FT, station measurements are expected to probe the regional FT at an elevation between z_t and the station elevation of 2225 m MSL. Comparisons to nearby aircraft O₃ soundings, available for 4 days of the study, were consistent with this expectation and confirmed that MBL air was not sampled.

[69] BUF or a combination of buoyant and mechanical (B&M) upslope flow occurred on approximately 39% of the summer days (or 16% of the hours) studied. The absence of significant BUF on the other 61% of the summer days is in sharp contrast to Mauna Loa Observatory (MLO) and Izaña where BUF is important on most days and all midday observations are typically discarded. During days on which BUF occurred, characteristic diurnal cycles of vertical wind speed, wind direction, and near-surface stability were observed. On average, BUF began shortly after sunrise on the western slope (0948 UTC). By 1100–1200 UTC, BUF was fully developed and vertical wind speeds were relatively constant at $\sim 0.8 \text{ m s}^{-1}$. Vertical wind speeds became negative around 2100 UTC with the transition to nighttime downslope flow. BUF caused the formation of orographic clouds on the mountain slope, but they generally did not extend all the way to the mountaintop. Uplift resulted in a diurnal cycle of specific humidity q_v at all stations. However, the daytime increase at the summit was small relative to that observed at MLO ($\sim 20 \text{ K}$ [Hahn *et al.*, 1992, Figure 12]), with a mean difference of the day-night dew point temperature extrema at Pico $\sim 13 \text{ K}$. In addition, the daytime enhancement in q_v at the summit was less than that on the slope, indicating a partial vertical separation of air masses that must limit the vertical range of upslope flow.

[70] On most BUF and B&M days, there was no evidence of significant impacts of uplift on station chemical measurements (except for concentrations of isoprene). In particular, afternoon enhancements in CO and NO_y were not significant, in contrast to observations at Izaña [Fischer *et al.*, 1998], and the afternoon decline in O₃ was small and not significant, in contrast to MLO [Hahn *et al.*, 1992; Ryan, 1997]. In 2005, isoprene (here used as a tracer for air originating below 1500 m msl) and *n*-butane (expected to be a tracer for anthropogenic air from sea level) measurements confirmed that upslope flow frequently occurs during May–August, but rarely transports air from low elevations to the PICO-NARE station. However, upslope flow carrying

island pollution or emissions from the station's generator (located 975 m lower) may have been observed on 1 day in 2004, when MBL height was only $\sim 300 \text{ m}$ below station elevation. This demonstrates the importance of carefully inspecting (or discarding) measurements during days affected by BUF.

[71] These findings are in contrast to the frequent influence of MBL air at the MLO and Izaña observatory. This may initially seem surprising, considering that relative to the PICO-NARE station MLO is more than 1 km higher, and Izaña is near the same elevation. There are several differences that likely contribute to the different behavior at Pico. Summertime inversion heights at Mauna Loa ($\sim 2\text{--}2.6 \text{ km}$ [Ryan, 1997]) are higher than they are at Pico, while those at Izaña are similar to those at Pico [Rodríguez *et al.*, 2004]. Thus the uplift required to bring MBL air to Pico during summer is similar to that required at MLO and Izaña, despite Pico's elevation. Most importantly, Pico Island is at a higher latitude (38° , versus 19° at MLO and 28° at Izaña). Lower insolation rates at Pico's higher latitude and the steep slope of Pico Mountain result in less solar heating (i.e., weaker buoyant forcing), and this difference is amplified by the relatively small size of Pico Island, which causes a weaker sea breeze. Indeed, buoyant forcing at Pico is nearly absent during winter, while it remains important at the more southerly stations year round. In contrast, mechanically forced upslope flow is more important at Pico, as a result of its relatively low elevation and higher synoptic wind speeds in the Azores region. These differences between Pico and two other volcanic island mountaintop stations highlight the need for station-specific evaluation of the roles played by both buoyant and mechanically driven upslope flow at such stations.

[72] These findings have important implications for the interpretation of measurements at the PICO-NARE station. Periods of strong mechanically driven upslope flow, when the dividing streamline height is within the MBL, should be excluded when station measurements are used to characterize the regional lower FT. (Since such periods are relatively common during winter, it may be possible to use them to characterize the wintertime local MBL, if the degree to which unmodified MBL air is sampled can be characterized in a future study.) The dividing streamline heights calculated using equation (2) provide a lower limit for the altitude effectively sampled by station measurements during all periods when BUF is not indicated. This lower limit is typically within 500 m of station altitude during summer, but is often lower during other seasons.

[73] During summers when mountainside meteorological measurements are not available the potential for BUF can be estimated using data from isoprene measurements and/or numerical weather prediction models. BUF was found to be most likely on days with downwelling shortwave radiation at the surface greater than 750 W m^{-2} and synoptic wind speeds near 850 hPa less than 8 m s^{-1} . This method successfully identified most days on which midday isoprene peaks were observed during spring and summer 2005.

[74] **Acknowledgments.** The authors wish to thank Katherine Strojny for TinyOS programming the Crossbow Mica2 nodes. The authors gratefully acknowledge funding from NOAA Climate and Global Change program grants NA16GP1658, NA03OAR4310002, and NA03OAR4310072 and NSF grants ATM-0215843 and INT-0110397.

We thank Marc Parlange for providing some of the micrometeorological instrumentation. Ozone measurements near Pico were obtained by the UK FAAM (Facilities for Airborne Atmospheric Instruments) BAe-146 aircraft and provided via the British Atmospheric Data Centre as part of the UK NERC (Natural Environment Research Council) funded project ITOP (Intercontinental Transport of Ozone and Precursors). ECMWF ERA-40 and operational model data used in this study have been obtained from the ECMWF data server by Diamantino Henriques from the Portuguese Meteorological Institute.

References

- Carbone, R., W. Cooper, and W.-C. Lee (1995), Forcing of flow reversal along the windward slopes of Hawaii, *Mon. Weather Rev.*, *123*, 3466–3480.
- Chen, Y.-L., and A. Nash (1994), Diurnal variations of surface airflow and rainfall frequencies on the island of Hawaii, *Mon. Weather Rev.*, *122*, 34–56.
- Ding, L., R. Calhoun, and R. Street (2003), Numerical simulation of strongly stratified flow over a three-dimensional hill, *Boundary Layer Meteorol.*, *107*(1), 81–114.
- Draxler, R., and G. Rolph (2003), HYSPLIT (Hybrid Single-Particle Lagrangian Integrated Trajectory) model, NOAA Air Resour. Lab., Silver Spring, Md. (Available at <http://www.arl.noaa.gov/ready/hysplit4.html>)
- Durrant, D., and J. Klemp (1982), On the effects of moisture on the Brunt-Vaisala frequency, *J. Atmos. Sci.*, *39*, 2152–2158.
- Fehsenfeld, F., P. Daum, W. Leaitch, M. Trainer, D. Parrish, and G. Hübler (1996), Transport and processing of O₃ and O₃ precursors over the North Atlantic: An overview of the 1993 North Atlantic Regional Experiment (NARE) summer intensive, *J. Geophys. Res.*, *101*(D22), 28,877–28,891.
- Fischer, E., R. Talbot, J. Dibb, J. Moody, and G. Murray (2004), Summer-time ozone at Mount Washington: Meteorological controls at the highest peak in the northeast, *J. Geophys. Res.*, *109*, D24303, doi:10.1029/2004JD004841.
- Fischer, H., et al. (1998), Trace gas measurements during the Oxidizing Capacity of the Tropospheric Atmosphere campaign 1993 at Izaña, *J. Geophys. Res.*, *103*, 13,505–13,518.
- Furger, M., et al. (2000), The VOTALP Mesolcina Valley campaign 1996: Concept, background and some highlights, *Atmos. Environ.*, *34*, 1395–1412.
- Greenberg, J. P., D. Helmig, and P. R. Zimmerman (1996), Seasonal measurements of nonmethane hydrocarbons and carbon monoxide at the Mauna Loa Observatory during the Mauna Loa Observatory Photochemistry Experiment 2, *J. Geophys. Res.*, *101*, 14,581–14,598.
- Hahn, C. J., J. T. Merrill, and B. G. Mendonca (1992), Meteorological influences during MLOPEX, *J. Geophys. Res.*, *97*, 10,291–10,309.
- Hastenrath, S., and L. Greischar (2001), The North Atlantic Oscillation in the NCEP-NCAR reanalysis, *J. Clim.*, *14*, 2404–2413, doi:10.1175/1520-0442.
- Hübner, G., et al. (1992), Total reactive oxidized nitrogen (NO_x) in the remote Pacific troposphere and its correlation with O₃ and CO: Mauna Loa Observatory Photochemistry Experiment 1988, *J. Geophys. Res.*, *97*, 10,427–10,447.
- Hunt, J., and W. Snyder (1980), Experiments on stably and neutrally stratified flow over a model three-dimensional hill, *J. Fluid Mech.*, *96*, 671–704.
- Igarashi, Y., Y. Sawa, K. Yoshioka, H. Matsueda, K. Fujii, and Y. Dokiya (2004), Monitoring the SO₂ concentration at the summit of Mt. Fuji and a comparison with other trace gases during winter, *J. Geophys. Res.*, *109*, D17304, doi:10.1029/2003JD004428.
- Jenkins, G., P. Mason, W. Moores, and R. Sykes (1981), Measurements of the flow structure around Ailsa Craig, a steep, three-dimensional, isolated hill, *Q. J. R. Meteorol. Soc.*, *107*, 833–851.
- Jiang, Q. (2003), Moist dynamics and orographic precipitation, *Tellus, Ser. A*, *55*, 301–326.
- Jobson, B. T., D. D. Parrish, P. Goldan, W. Kuster, F. C. Fehsenfeld, D. R. Blake, N. J. Blake, and H. Niki (1998), Spatial and temporal variability of nonmethane hydrocarbon mixing ratios and their relation to photochemical lifetimes, *J. Geophys. Res.*, *103*, 13,557–13,567.
- Kleissl, J., R. E. Honrath, and D. Henriques (2006), Analysis and application of Sheppard's airflow model to predict mechanical orographic lifting and the occurrence of mountain clouds, *J. Appl. Meteorol.*, *45*(10), 1376–1387.
- Lewis, A., et al. (2006), Chemical composition observed over the mid-Atlantic and the longevity of pollution signatures far from source regions, *J. Geophys. Res.*, doi:10.1029/2006JD007584, in press.
- Mendonca, B. (1969), Local wind circulation on the slopes of Mauna Loa, *J. Appl. Meteorol.*, *8*, 533–541.
- Mendonca, B., and R. Pueschel (1973), Ice nuclei, total aerosol, and climatology at Mauna Loa, Hawaii, *J. Appl. Meteorol.*, *12*, 156–160.
- Oltmans, S. J., et al. (1996), Summer and spring ozone profiles over the North Atlantic from ozonesonde measurements, *J. Geophys. Res.*, *101*, 29,179–29,200.
- Oltmans, S. J., et al. (1998), Trends of ozone in the troposphere, *Geophys. Res. Lett.*, *25*, 139–142.
- Owen, R. C., O. R. Cooper, A. Stohl, and R. E. Honrath (2006), An analysis of the mechanisms of North American pollutant transport to the central North Atlantic lower free troposphere, *J. Geophys. Res.*, *111*, D23S58, doi:10.1029/2006JD007062.
- Parrish, D. D., M. Trainer, J. S. Holloway, J. E. Yee, M. S. Warshawsky, F. C. Fehsenfeld, G. Forbes, and J. L. Moody (1998), Relationships between ozone and carbon monoxide at surface sites in the North Atlantic region, *J. Geophys. Res.*, *103*, 13,357–13,376.
- Peterson, M. C., R. E. Honrath, D. D. Parrish, and S. J. Oltmans (1998), Measurements of nitrogen oxides and a simple model of NO_x fate in the remote North Atlantic marine atmosphere, *J. Geophys. Res.*, *103*, 13,489–13,503.
- Rasmussen, R., P. Smolarkiewicz, and J. Warner (1989), On the dynamics of Hawaiian cloud bands: Comparison of model results with observations and island climatology, *J. Atmos. Sci.*, *46*, 1589–1606.
- Ridley, B., and E. Robinson (1992), The Mauna Loa Observatory Photochemistry Experiment, *J. Geophys. Res.*, *97*, 10,285–10,290.
- Ridley, B. A., E. L. Atlas, J. G. Walega, G. L. Kok, T. A. Staffelbach, J. P. Greenberg, F. E. Grahek, P. G. Hess, and D. D. Montzka (1997), Aircraft measurements made during the spring maximum of ozone over Hawaii: Peroxides, CO, O₃, NO_x, condensation nuclei, selected hydrocarbons, halocarbons, and alkyl nitrates between 0.5 and 9 km altitude, *J. Geophys. Res.*, *102*, 18,935–18,961.
- Rodriguez, S., C. Torres, J.-C. Guerra, and E. Cuevas (2004), Transport pathways of ozone to marine and free-troposphere sites in Tenerife, Canary Islands, *Atmos. Environ.*, *38*, 4733–4747.
- Ryan, S. (1997), The wind field around Mauna Loa derived from surface and balloon observations, *J. Geophys. Res.*, *102*, 10,711–10,725.
- Scheel, H. E., E.-G. Brunke, R. Sladkovic, and W. Seiler (1998), In situ CO concentration at sites Zugspitze (47°N, 11°E) and Cape Point (34°S, 18°E) in April and October 1994, *J. Geophys. Res.*, *103*, 19,295–19,304.
- Schmitt, R., and A. Volz-Thomas (1997), Climatology of ozone, PAN, CO, and NMHC in the free troposphere over the southern North Atlantic, *J. Atmos. Chem.*, *28*, 245–262.
- Serviço Regional de Estatística dos Açores (2005), Anuário Estatístico da Região Autónoma dos Açores, Ponta Delgada, Azores, Portugal.
- Sheppard, P. (1956), Airflow over mountains, *Q. J. R. Meteorol. Soc.*, *82*, 528–529.
- Smith, R. (1988), Linear theory of stratified flow past an isolated mountain in isosteric coordinates, *J. Atmos. Sci.*, *45*, 3889–3896.
- Snyder, W. (1985), Fluid modeling of pollutant transport and diffusion in stably stratified flows over complex terrain, *Annu. Rev. Fluid Mech.*, *17*, 239–266.
- Spangler, T. (1987), Comparison of actual dividing-streamline heights to height predictions using the Froude-number, *J. Clim. Appl. Meteorol.*, *26*(1), 204–207.
- Tanner, D., D. Helmig, J. Hueber, and P. Goldan (2006), Gas chromatography system for the automated, unattended, and cryogen-free monitoring of C₂ to C₆ non-methane hydrocarbons in the remote troposphere, *J. Chromatogr. A*, *1111*, 76–88.
- Taylor, P., and H. Teunissen (1987), The Askervein hill project: Overview and background data, *Boundary Layer Meteorol.*, *39*, 15–39.
- Tsutsumi, Y., Y. Zaizen, and Y. Makino (1994), Tropospheric ozone measurement at the top of Mt. Fuji, *Geophys. Res. Lett.*, *21*, 1727–1730.
- Val Martín, M., R. E. Honrath, R. C. Owen, and G. Pfister (2006), Significant enhancements of nitrogen oxides, black carbon, and ozone in the North Atlantic lower free troposphere resulting from North American boreal wildfire, *J. Geophys. Res.*, *111*, D23S60, doi:10.1029/2006JD007530.
- Vosper, S., I. Castro, W. Snyder, and S. Mobbs (1999), Experimental studies of strongly stratified flow past three-dimensional orography, *J. Fluid Mech.*, *390*, 223–249.
- Walega, J. G., et al. (1992), Observations of peroxyacetyl nitrate, peroxypropionyl nitrate, methyl nitrate and ozone during the Mauna Loa Observatory Photochemistry Experiment, *J. Geophys. Res.*, *97*, 10,311–10,330.
- Whiteman, C. (2000), *Mountain Meteorology: Fundamentals and Applications*, Oxford Univ. Press, New York.
- Whiteman, C. D. (1990), Observations of thermally developed wind systems in mountainous terrain, in *Atmospheric Processes Over Complex Terrain, Meteorol. Monogr.*, vol. 23, edited by W. Blumen, pp. 5–24, Am. Meteorol. Soc., Boston, Mass.

Wilczak, J., S. Oncley, and S. Stage (2001), Sonic anemometer tilt correction algorithms, *Boundary Layer Meteorol.*, *99*, 127–150.

Zanis, P., E. Schuepbach, H. Scheel, M. Baudenbacher, and B. Buchmann (1999), Inhomogeneities and trends in the surface ozone record (1988–1996) at Jungfraujoch in the Swiss Alps, *Atmos. Environ.*, *33*, 3777–3786.

D. Helmig and D. Tanner, Institute of Arctic and Alpine Research, University of Colorado, Boulder, CO 80309, USA.

J. Kleissl, Department of Mechanical and Aerospace Engineering, University of California, San Diego, La Jolla, CA 92093, USA. (jan@kleissl.com)

M. P. Dziobak, R. E. Honrath, R. C. Owen, and M. Val Martín, Department of Civil and Environmental Engineering, Michigan Technological University, Houghton, MI 49931-1295, USA. (reh@mtu.edu)